Conformational Analysis of Model Poly(ether urethane) Chains in the Unperturbed State and under External Forces

İskender Yılgör,† Ersin Yurtsever,† and Burak Erman*,†,‡

Chemistry and Mechanical Engineering Departments, Koç University, Sariyer 80910, İstanbul, Turkey

Received July 29, 2002; Revised Manuscript Received October 16, 2002

ABSTRACT: Conformational features of model poly(ether urethane) (PEU) single chains are investigated in the unperturbed state and under external force. Model PEUs consisting of symmetrical, aromatic, 1,4-phenylene diisocyanate (PDI) hard segments and poly(tetramethylene oxide) (PTMO) soft segments with varying lengths are considered. Rotational potential maps are calculated quantum mechanically using the AM1 parametrization with Gaussian98. Configurations of the chains are generated by the Monte Carlo technique, using the rotational isomeric state formalism and successive matrix multiplication scheme. Unperturbed dimensions, the change in dimensions when a force acts along the end-to-end vector, the stiffness, and toughness of the chain and orientability of segments under external force are characterized and compared with properties of polyethylene. The characteristic ratio of a long PEU chain is 5.0, and the Kuhn length for a single block is 9.2 Å, both of which are smaller than the corresponding polyethylene values. The model chains are significantly more ductile and tougher than polyethylene. The orientability of the backbones exhibits a strong even−odd effect, with strongly orientable bonds neighbored by weakly orienting ones. The degree of rigidity of the phenyl group does not propagate far along the chain. The projection of the bond vectors on the phenyl axis decay rapidly with increasing distance of the bond along the chain.

Introduction

Linear, segmented polyurethanes constitute one of the most interesting classes of multiphase copolymer systems. Interesting properties and performance of segmented thermoplastic polyurethane and polyurethaneurea copolymers are strongly dependent on their chemical structures and resulting microphase morphologies. Microphase morphologies of polyurethanes or polyureas are determined by several factors. These include the extent of competitive hydrogen bonding between hard−hard and hard−soft segments, the structure and crystallizability of the hard segments, inherent solubility between hard and soft segments, and nature of the interdomain interface between phases and related free energy and entropy changes.[1−3] There is an ever-increasing interest in these systems for many different reasons. These include (i) synthetic efforts for the preparation of well-defined backbone structures,[4,5] (ii) studies on understanding the influence of hydrogen bonding and segment crystallization on their morphological behavior,[6−8] (iii) investigations on the influence of sample preparation methods and thermal history on phase separation,[9,10] (iv) studies in understanding the structure−morphology−property relations,[11−13] and (v) processing behavior[14] and industrial applications.[15]

In addition to experimental investigations, there have been several theoretical studies on segmented polyurethanes and related model systems in order to understand the fundamentals of their structure−property relationships better. These studies included semiempirical and advanced quantum mechanical calculations on the determination of hydrogen-bonding interactions between hard and soft segments,[8,13] ab initio characterizations of molecular structures and conformation energies,[16] and determination of the vibrational spectra and modeling the chain conformation and packing of hard segments[17,18] in polyurethane elastomers.

In this study, we investigate the conformational features of model poly(ether urethane) (PEU) single chains in the unperturbed state and under external forces. Model PEUs consist of very symmetrical, 1,4-phenylene diisocyanate hard segments and poly(tetramethylene oxide) (PTMO) soft segments with varying lengths. A representative portion of the chain is shown in Figure 1, and its structure is described in detail in the following section. In the present work, the conformational properties of the single chain are investigated. The analysis gives information on the intramolecular features of the chain. Among these are the unperturbed dimensions, the change in dimensions when a force acts along the end-to-end vector, the stiffness, toughness of the chain, orientability of segments under external force, etc. The study of these features is important because many of the structure−property relations of polymers in the bulk state are derived in an additive manner from the single chain properties.[19,20] A quantitative evaluation of these properties also allows for comparison of the polyurethanes with other molecules whose properties are better characterized. In the present study, we compare the results of calculations with those for the polyethylene chains.

Since only single chains are investigated, effects of intermolecular nature, i.e., the interaction of the chain with its environment such as hydrogen bonding of various units with other chains and dimensional changes resulting from interactions with the environment, are not covered in the present paper. It is possible to study these effects for the single chain and the bulk state model systems by molecular dynamics, and work is in progress in our laboratories.

In addition to theoretical studies, these types of model PEUs have also been successfully synthesized in our

† Chemistry Department.
‡ Mechanical Engineering Department.
* Corresponding author. e-mail: berman@ku.edu.tr.

10.1021/ma021217b CCC: $22.00
Published on Web 11/12/2002

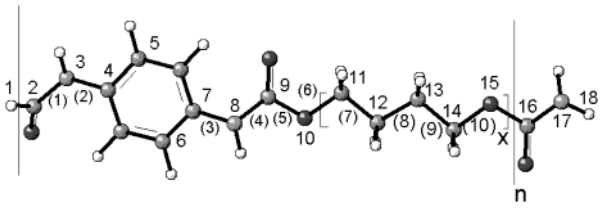

Figure 1. Chemical structure of the chain. The repeating block of the molecule is between the two vertical lines. The number of repeating blocks is represented by *n*, which is varied between 1 and 24 in the present calculations. The polyether group shown between the squared brackets repeats *x* times within each block. *x* is chosen as 14 in the present study. The numbers on the various atoms are used for identifying the various bond and torsional angles.

Table 1. Bond Lengths and Bond Angles

bond *ij*	bond length, l_{ij} (Å)	bond angle, θ_{ijk}	value of bond angle (deg)
2−3	1.38	1−2−3	112.2
3−8	5.76	2−3−4	127.8
8−9	1.38	7−8−9	125.4
9−10	1.38	8−9−10	111.1
10−11	1.44	9−10−11	114.8
11−12	1.52	10−11−12	105.5
12−13	1.51	11−12−13	109.8
13−14	1.51	12−13−14	109.8
14−15	1.44	13−14−15	105.6
15−16	1.38	14−15−16	114.6
16−17	1.37	15−16−17	113.2

laboratories. Their physicochemical characterization and their structure−property relations are underway and will be reported later.

Formulation and Simulations

Structure of the Chain. In Figure 1, the chemical structure of the chain is shown. The repeating block of the molecule is shown between the two vertical lines. The number of repeating blocks is represented by *n*, which is varied between 1 and 24 in the present calculations. The polyether group shown between the squared brackets also repeats *x* times within each block. In the present model chain, *x* is taken as 14. Experimental analysis, to be reported, of the various length model polyurethanes showed that the value of $x = 14$ and $n \geq 20$ yields materials with excellent mechanical properties. The numbers on the various atoms shown in the figure are used for identifying the various bond and torsional angles, as described in detail below. The bond lengths used in the calculations are given in the second column of Table 1. The first column gives the number of the backbone atoms, *i* and *j*, at the two extremities of the bond, and the second column gives the bond length, l_{ij}, in angstroms. The various bond angles used in the calculations are given in the third and fourth columns of Table 1, where the third column gives the three atoms that identify the bond angle, and the fourth column gives the value of the bond angle, in degrees. The bond lengths and angles given in Table 1 are those obtained from full optimization using the software Gaussian98, described in more detail in the following paragraph.

Ten torsional angles are used for identifying the configurations of the block, and are given in Table 2, according to Flory notation[19] where the first column numbers each torsional angle, from 1 to 10, and the second column gives the four atoms that define the angle.

Table 2. Torsional Angles

torsional angle, *i*	four atoms that define the angle *i*	torsional angle, *i*	four atoms that define the angle *i*
1	1−2−3−4	6	9−10−11−12
2	2−3−4−5	7	10−11−12−13
3	6−7−8−9	8	11−12−13−14
4	7−8−9−10	9	12−13−14−15
5	8−9−10−11	10	13−14−15−16

The rotational potential maps are calculated quantum mechanically using[21] the AM1 parametrization with Gaussian98, revision A6. In each map, the rotational space of two successive torsional angles, $i - 1$ and i, have been spanned by 15° increments while optimizing all other geometrical parameters including bond lengths and valence angles. The initial structures assume anti positions (180°) for all other torsional angles along the backbone. The energies corresponding to each pair of torsional angles $i - 1$ and i are plotted in the form of contour diagrams. Four representative maps showing the results of calculations are presented in Figure 2a−d for bond pairs 1−2, 3−4, 4−5, and 5−6. The bond $i - 1$ is represented along the abscissa and the bond i along the ordinate. Maps for the remaining bond pairs are also obtained to generate the energy data for the calculations but not presented to economize from space. Locations of rotational isomeric minima and the corresponding energies obtained from all of the maps needed for the present calculations are presented in Table 3. The first two columns give the values of the torsional angles $i - 1$ and i, and the third column gives the corresponding energy in kcal/mol. For states with high energy values, a value of 7.0 kcal/mol is adopted as shown in Table 3. This allows for the appearance of the corresponding isomeric state in the rotational isomeric state formalism but with negligibly small frequency. For $x > 1$, the oxygen atom at the terminus of the repeat unit is connected to a CH_2 unit, which makes the bonds 9, 10, and 11 equivalent to those in the poly(ethylene oxide) chain. The torsional energies about the bonds 9−10 and 10−11 (where bond 11 is the O−CH_2 bond) shown in Table 3 are taken from Mark and Flory.[22]

Generation of Chain Conformations According to the Rotational Isomeric State Formalism. Configurations of the chains are generated according to the rotational isomeric state formalism and successive matrix multiplication scheme. Accordingly, the end-to-end vector for any given conformation of a block of *N* bonds is expressed as[23]

$$\mathbf{r} = \mathbf{A}_{[1}[\prod_{i=2}^{N-1}\mathbf{A}_i]\mathbf{A}_{N]} \tag{1}$$

where $\mathbf{r}$ is the end-to-end vector, and

$$\mathbf{A}_{[1} = [\mathbf{T}_1 \;\; \mathbf{l}_1], \quad \mathbf{A}_i = \begin{bmatrix} \mathbf{T}_i & \mathbf{l}_i \\ \mathbf{0} & 1 \end{bmatrix}, \quad \mathbf{A}_{N]} = \begin{bmatrix} \mathbf{l}_N \\ 1 \end{bmatrix} \tag{2}$$

Here, $\mathbf{T}_i$ is the transformation matrix for the *i*th bond, $\mathbf{l}_i$ is the *i*th bond vector, expressed in the coordinate frame of the bond, and $\mathbf{0}$ is the row vector, [0 0 0]. The end-to-end vector is expressed with respect to the external coordinate system chosen as follows: The *x*-axis is directed along the first bond between atoms 2 and 3 of Figure 1. The torsional angle of the first bond is kept fixed at 0°. The *y*-axis is chosen in the plane defined by the bonds 1 and 2. The *z*-axis is chosen to complete a right-handed system. The data required to construct the

Table 3. Isomeric States and Corresponding Energies

map $i-1, i$	ϕ_{i-1}	ϕ_i	energy (kcal/mol)
map 12	−180	−165	0
	−180	0	0.04
	−180	165	0
	0	−180	1.44
	0	0	0.99
	0	180	1.44
	180	−165	0
	180	0	0.04
	180	165	0
map 34	−165	−180	1.85
	−180	0	0.45
	−165	180	1.85
	0	−180	1.68
	0	0	0
	0	180	1.68
	165	−180	1.86
	180	0	0.45
	165	180	1.86
map 45	−180	−180	7.00
	−180	0	1.56
	−180	180	7.00
	0	−180	2.34
	0	0	0.11
	0	180	2.34
	180	−180	7.00
	180	0	1.56
	180	180	7.00
map 56	−180	−105	4.30
	−180	0	4.40
	−180	105	4.31
	0	−105	0.02
	0	0	0.27
	0	105	0
	180	−105	4.30
	180	0	4.40
	180	105	4.31
map 67	−105	−105	7.0
	−105	0	0.02
	−105	105	7.00
	0	−105	0.60
	0	0	0.26
	0	105	0.48
	105	−105	7.00
	105	0	0
	105	105	0.47
map 78	−105	−105	1.34
	−105	0	1.12
	−105	105	0
	0	−105	0.90
	0	−15	0.55
	0	105	1.12
	105	−105	7.0
	105	0	0.90
	105	105	7.0
map 9−10	−120	−120	1.00
	−120	0	0.00
	−120	120	1.38
	0	−120	1.38
	0	0	0.40
	0	120	1.38
	120	−120	1.38
	120	0	0.00
	120	120	1.00
map 10−11	−120	−120	2.00
	−120	0	1.00
	−120	120	7.00
	0	−120	1.00
	0	0	0.00
	0	120	1.00
	120	−120	7.00
	120	0	1.00
	120	120	2.00

A matrices, i.e., the bond lengths, bond angles, and the torsional angles representing the isomeric minima, are shown in Tables 1−3.

According to the Monte Carlo scheme, a configuration of the chain is generated by choosing the set of torsional states (angles) that defines the specific configuration.

Each energy map for a pair of bonds $\zeta\eta$ shown in Figure 2 is obtained by allowing all the remaining bonds to assume every possible configuration. The joint probability that bond $i-1$ is in state ζ and the ith bond is in state η, when all other bonds take all possible configurations subject to the bond torsional energies, is obtained from the expression

$$p_{\zeta\eta;i} = Z^{-1}J^*[\prod_{h=2}^{i-1}U_h]\frac{\partial U_{\zeta\eta;i}}{\partial \ln u_{\zeta\eta;i}}[\prod_{j=i+1}^{N-1}U_h]J \qquad (3)$$

where the index i comprises all n bonds of the sequence shown in Figure 1, $U_{\zeta\eta;i}$ are the components of the statistical weight matrix given by

$$U_{\zeta\eta;i} = \exp(-E_{\zeta\eta;i}/RT) \qquad (4)$$

$J^* = [1\ 0\ 0\ ]$, $J = \mathrm{col}\ [\ 1\ 1\ 1]$, and the partition function Z is calculated according to

$$Z = J^*[\prod_{i=2}^{N-1}U_i]J \qquad (5)$$

The values of the energies used in eqs 3−5 and the corresponding torsional angles are given in Table 3. During the Monte Carlo generation of the chain, the choice of the state of the ith bond when the $(i-1)$st bond is already chosen to be in state ζ is made according to the conditional probability, $q_{\zeta\eta;i}$, defined as

$$q_{\zeta\eta;i} = \frac{p_{\zeta\eta;i}}{\sum_{\eta=1}^{3}p_{\zeta\eta;i-1}} \qquad (6)$$

The matrices $p_{\zeta\eta;i}$ and $q_{\zeta\eta;i}$ are not given in the present paper due to size considerations but are available on request. Each block shown in Figure 1 is joined to the following block with an OC bond, shown as the bond 15−16. This bond is always in the trans state due to its partial double-bond character. For the Monte Carlo calculation of dimensions of a given block, the product $[\prod_{i=2}^{N-1}A_i]$ given by the square brackets of eq 1 is formed for 10^5 random configurations of the block. All of the 10^5 values of this product are stored. The end-to-end vector of a chain of n blocks is obtained by the serial multiplication of the products of the stored random **A** matrices. For example, for three blocks, the end-to-end vector is obtained as

$$\mathbf{r} = \mathbf{A}_{[1}[\prod_{i=2}^{N-1}\mathbf{A}_i][\prod_{i=2}^{N-1}\mathbf{A}_i][\prod_{i=2}^{N-1}\mathbf{A}_i]\mathbf{A}_{N]} \qquad (7)$$

where the term in each bracket is chosen randomly from among the stored 10^5 matrices.

Distribution Functions for Model Chains in the Free State and under a Stretching Force. The distribution function for a chain with a force **f** acting on its both ends is given as[19]

$$W_f(r) = W(r)\exp(\mathbf{f}\cdot\mathbf{r}/kT) \qquad (8)$$

where $W(r)$ is the distribution function for a free chain

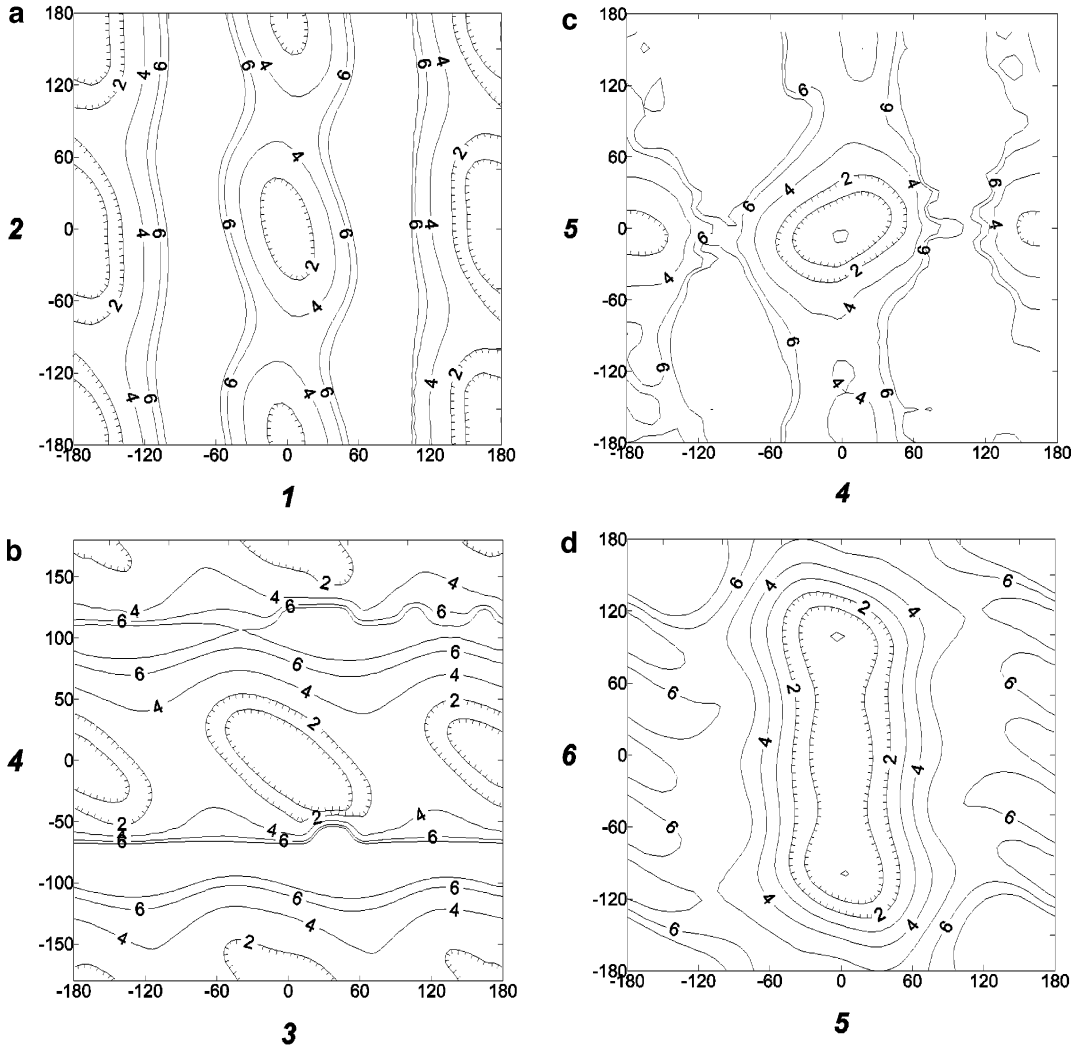

Figure 2. (a) Contour map for torsional energies of the first and second bonds. The angles are given according to Flory representation,[19] 0^0 representing the trans state. The abscissa and ordinate values are for the first and second bonds, respectively. (b) Contour map for torsional energies of the third and fourth bonds. See legend for (a). (c) Contour map for torsional energies of the fourth and fifth bonds. See legend for (a). (d) Contour map for torsional energies of the fifth and sixth bonds. See legend for (a).

whose end-to-end distance is r. In the present calculations $W(r)$ is obtained by partitioning the calculated scalar end-to-end distances obtained at each Monte Carlo generation into forty intervals between $r = 0$ and r_{max}.

The squared average of the end-to-end distance, $\langle r^2 \rangle$, when the chain is under a force **f** is obtained from eq 8 as

$$\langle r^2 \rangle = \sum_i r_i^2 W_f(r_i) \tag{9}$$

where the subscript i refers to the ith interval. Thus, r_i is the value of the end-to-end distance corresponding to the midpoint of the ith interval, and $W_f(r_i)$ is the corresponding value of the distribution function. Each average reported below is based on 100 000 chain configurations.

Results and Discussion

In this section, we present results of calculations for the model poly(ether urethane) chains. We compare various statistical features of the chains with those of the widely studied polyethylene chains. The parameters used for the polyethylene chain are those given by Flory.[19]

Unperturbed Dimensions. The mean-squared end-to-end distance for an unperturbed block ($n = 1$) at 300 K is 960 Å^2 , calculated according to eq 9 with $f = 0$. The characteristic ratio for a single block is calculated as $C_n = \langle r^2 \rangle / nl^2 = 5.0$. The same value of C_n is obtained for chains up to 24 blocks, indicating that this value is indeed the converged value; i.e., $C_\infty = 5.0$ for this system. A polyethylene chain equivalent to one block contains about 81 bonds having a bond length of 1.54 Å each. The characteristic ratio C_∞ equates to 6.9 for polyethylene. The smaller value for the polyurethane chain results mainly from the presence of the backbone oxygens. Inspection of the energy maps indicates that when bond 5 is in the trans state, rotations about bond 6 are unhindered. The elements of the joint probability matrix $p_{\zeta\eta;6}$, obtained by using eq 3, where ζ and η show the states of the 5th and 6th bonds are

$$p_{\zeta\eta;6} = \begin{array}{c} \\ g^+ \\ t \\ g^- \\ \\ \end{array} \begin{array}{c} \begin{array}{ccc} g^- & t & g^+ \end{array} \\ \begin{bmatrix} 0.00 & 0.00 & 0.00 \\ 0.322 & 0.276 & 0.402 \\ 0.00 & 0.00 & 0.00 \end{bmatrix} \end{array}$$

Thus, bond 5 is always in the trans state, and bond 6, although its gauche$^+$ state is more favored to its trans state, may be approximated by the freely rotating bond.

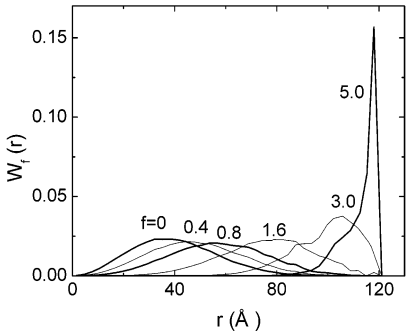

Figure 3. Distribution of the end-to-end distance for different values of the force, *f*, for a model chain having two repeat blocks. The force values shown on each curve are given in piconewtons.

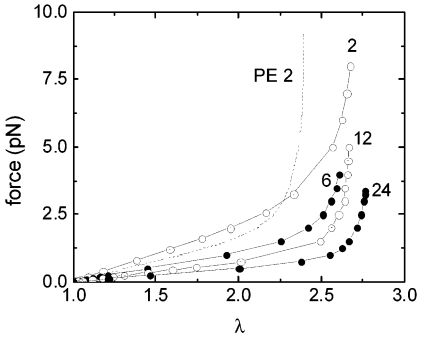

Figure 4. Force vs extension ratio curves. The extension ratio λ given along the abscissa is defined as the square root of the ratio of perturbed and unperturbed mean-squared end-to-end vector. The numbers on each curve denote the number of blocks. The circles show results of calculations, and the lines are interpolations through the points. Results for a polyethylene chain of 160 bonds equivalent to a model chain of two blocks are also shown in the figure with the dashed curve.

The fully stretched length, l_{max}, of one block is ca. 104 Å. The Kuhn length, l_K, given by the expression $l_K = \langle r^2\rangle_0/l_{max}$ is 9.2 Å, which, despite the presence of the backbone phenyl group, is smaller than $l_K = 12$ Å for polyethylene. The number, N_K, of Kuhn segments in one block of the PEU chain, obtained according to the expression $N_K = l_{max}^2/\langle r^2\rangle_0$, is 11. A polyethylene chain of this length has $N_K = 9.2$.

Transformation of the Distribution Function under Force. In Figure 3, the distribution of the end-to end distance is presented for different values of the force, *f*, for a model chain having two repeat blocks. The force shown on each curve is in piconewtons. For clarity, the curves corresponding to 0.4, 1.6, and 3.0 pN are shown by thinner lines to distinguish from the others. The maxima of the distribution curves remain approximately constant at low to moderate force values, but they are shifted to larger *r* values. At high values of force, the width of the distribution decreases significantly, leading to a sharp peak. It should be noted that the fully stretched end-to-end distance of the chain with two blocks is about 200 Å, whereas the largest force, 5 pN, applied to the chain stretches it up to 120 Å, as seen from Figure 3. The reason for this is that when $f = 0$, i.e., the unperturbed state, the chains are highly coiled and there are very few chains with $r > 120$, as seen from Figure 3. When a force is applied, the distribution is multiplied by $\exp[\mathbf{f}'\mathbf{r}/kT]$, which changes the probability of the chains that exist in the unperturbed ensemble.

Force−Extension Curves. In Figure 4, force vs extension ratio curves are presented. The extension ratio λ is defined as the square root of the ratio of perturbed and unperturbed mean-squared end-to-end vector. Calculations are performed for model chains of different lengths, indicated by the numbers on the curves. The circles indicate results of calculations, according to which a force is chosen, and the mean-squared end-to-end distance is evaluated using eq 9. Results for a polyethylene chain of 160 bonds at 300 K, which is equivalent to a model polyurethane chain of two blocks, are also shown in the figure with the dashed curve. The slopes of the initial portions of the curves for PE and PEU, which indicate the linear spring constant of the respective chains, are 0.058 and 0.085, respectively, indicating that the model chain is stiffer than the PE chain in the linear regime. Despite the presence of CO bonds along the chain, which are expected to make the chain softer, this enhanced stiffness results perhaps from the presence of several other bonds whose rotations are strongly restricted, as may be verified by the inspection of the energy maps. However, the extensibility or the "ductility" of the model chain is larger, and it is significantly tougher than PE. The area under the diagram is 0.14 for PEU, while it is 0.08 for PE.

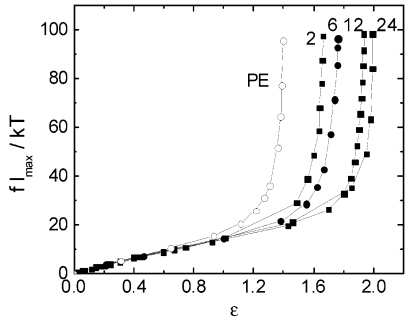

Figure 5. Scaling of the force with strain. Filled symbols represent results of calculations for different length chains. Open circles are for a PE chain of 160 bonds. The curves are obtained by interpolation through the calculated curves.

Scaling of Chain Dimensions under Force. The variables involved in the problem of chain stretching are (i) maximum length, l_{max}; (ii) mean-squared chain dimensions, $\langle r^2\rangle_0$ in the unperturbed state and $\langle r^2\rangle$ in the perturbed state; (iii) force, *f*; and (iv) temperature, *kT*. The unperturbed and perturbed dimensions may be joined into a single term by defining a strain term, $\epsilon = (\langle r^2\rangle^{1/2} - \langle r^2\rangle_0{}^{1/2})/\langle r^2\rangle_0{}^{1/2}$. Thus, there are four variables, l_{max}, *f*, ϵ, and *T*, and two dimensions (force and length). Applying dimensional analysis to the problem,[25] we can show that the force deformation relations can be expressed in terms of two dimensionless variables. We choose these two variables as $f\,l_{max}/kT$ and ϵ. It is then possible to write a relation

$$f\,l_{max}/kT = a\epsilon^{\beta} \tag{10}$$

where *a* is the front factor and β is the exponent. In Figure 5, the left-hand side of eq 10 is plotted as a function of ϵ for model chains of different lengths with number of blocks varying between 2 and 24. Filled points are for the model chains of various numbers of blocks. In the same figure, results for PE of 160 repeat units are also plotted using open circles. All of the curves collapse into a straight line for strains in the range $0 < \epsilon < 1$. The front factor *a* equates to 14 from the figure, and the exponent β is unity. The latter results from the

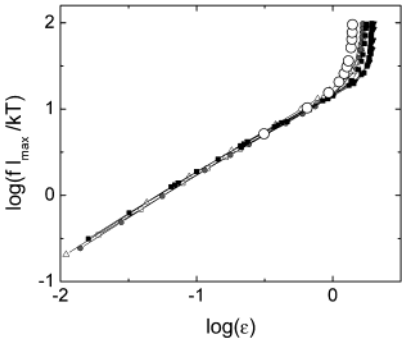

Figure 6. A log−log plot of Figure 5.

fact that the chains are subject to local intramolecular forces, and excluded-volume effects and long-range interactions are not included in the calculations. To see the range of validity of the scaling arguments used in obtaining this figure, a log−log plot is presented in Figure 6, indicating the collapse of the data points onto a single curve, including that of PE (open circles). The deviation of the curves from a straight line at higher extensions indicates that the finite extensibility features of the chains have not been represented sufficiently well in the expression given by eq 10 and that additional variables are needed in the scaling argument.

Orientation of Chain Segments under Force. For sufficiently long chains, the orientation of a given segment of the chain whose ends are fixed at r may be expressed in terms of the mean-squared cosine of the angle Φ_i which the bond makes with the end-to-end vector r:[19]

$$\langle \cos^2 \Phi_i \rangle_r = \frac{1}{3} + \frac{1}{5}\left[\frac{3\langle r^2 \cos^2 \Phi_i \rangle_0}{\langle r^2 \rangle_0} - 1\right]\frac{r^2}{\langle r^2 \rangle_0} \quad (11)$$

Here, the averages with the subscript zero are taken for the free chain. The subscript r on the left-hand side indicates that the term in the angular brackets is for a chain at fixed r. Averaging both sides of eq 11 over all possible values of r leads to the expression

$$S = \frac{3}{2} D_0 \lambda^2 \quad (12)$$

where S is the orientation function, $S = {}^1/_2(3\langle \cos^2 \Phi_i \rangle - 1)$, and D_0 is

$$D_0 = \frac{1}{5}\left[\frac{3\langle r^2 \cos^2 \Phi_i \rangle_0}{\langle r^2 \rangle_0} - 1\right] \quad (13)$$

Here, D_0 denotes the orientational susceptibility of the given bond to the deformation of the chain.We calculate D_0 for different bonds within a single block of the model PEU chain.[24] Results of calculations of D_0 for the single block according to eq 13 are shown in Figure 7. Filled circles are for PEU. For comparison, values for PE are also calculated and indicated by the empty circles. Results for only half of the block comprising bonds 3−44 are presented. The striking feature of the results is that the D_0 values exhibit a very strong even−odd effect for PEU that persists all along the chain. PE, on the other hand, exhibits a small degree of even−odd effect. In general, the odd-numbered bonds of PEU are about 1.5−2 times more orientable than PE. The even-numbered bonds of PEU, on the other hand, exhibit a

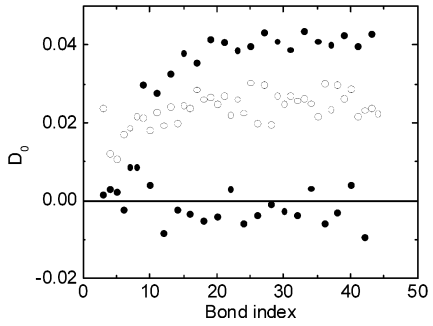

Figure 7. D_0 values for different bonds within a single block of the model PEU chain. Filled and open circles are for PEU and PE, respectively. Results for only half of the block comprising bonds 3−44 are presented.

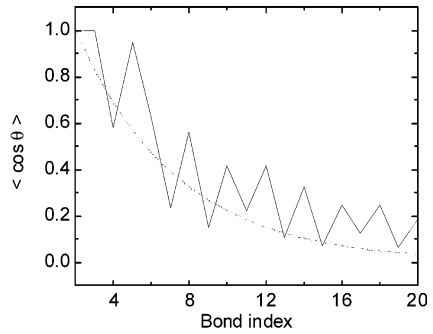

Figure 8. Projection of a given bond on the axis of the phenyl group along the chain. The abscissa values indicate the bond that is projected on the phenyl axis. The ordinate values denote the cosine of the angle between the bond and the axis, averaged over all configurations of the chain. The dashed curve is for a freely rotating chain.

negligible amount of orientation, alternating between negative and positive small values, as may be verified from Figure 7. Another feature observed from Figure 7 is that the odd-numbered bonds near the center of the PEU chain are more orientable than the ones closer to the end.

The present calculations are for the single chain and therefore do not contain information on the bulk features, such as the interaction of the rigid segment with its environment or the role of hydrogen bonds. Both of these features play important role in bulk properties of the PEU chains. The degree of rigidity imparted by the backbone phenyl group on the chain, however, is an intramolecular property and may be estimated by the single chain calculations. In Figure 8, we show the projection of a given bond on the axis of the phenyl group along the chain. The abscissa values indicate the bond that is projected on the phenyl axis. Ordinate values denote the cosine of the angle between the bond and the axis, averaged over all configurations of the chain. The dashed curve is calculated for a freely rotating chain. Comparison of the two curves shows that the stiffness imparted by the rigid phenyl group does not propagate far along the chain backbone. Apart from the strong even odd effects resulting from the local specific configurational features of the chain, the decay of the projections shown in Figure 8 is essentially the same as that of the freely rotating chain.

References and Notes

(1) Lelah, M. D.; Cooper, S. L. *Polyurethanes in Medicine*; CRC Press: Boca Raton, FL, 1986.
(2) Hepburn, C. *Polyurethane Elastomers*, 2nd ed.; Elsevier Applied Science: Amsterdam, 1991.

(3) Abouzahr, S.; Wilkes, G. L.; Ophir, Z. *Polymer* **1982**, *23*, 1077−1084.
(4) Yen, F.-S.; Lin, L.-L.; Hong, J.-L. *Macromolecules* **1999**, *32*, 3068−3079.
(5) Yilgor, E.; Yilgor, I. *Polymer* **2001**, *42*, 7953−7959.
(6) Brunette, C. M.; Hsu, S. L.; MacKnight, W. J. *Macromolecules* **1982**, *15*, 2215−2221.
(7) Ning, L.; De-Ning, W.; Sheng-Kang, Y. *Polymer* **1996**, *37*, 3577−3583.
(8) Yilgor, E.; Yurtsever, E.; Yilgor, I. *Polymer* **2002**, *43*, 6558−6566.
(9) Saiani, A.; Daunch, W. A.; Verbeke, H.; Leenslang, J. V.; Higgins, J. S. *Macromolecules* **2001**, *34*, 9059−9068.
(10) Garrett, J. T.; Lin, J. S.; Runt, J. *Macromolecules* **2002**, *35*, 161−168.
(11) Koberstein, J. T.; Galambos, A. F.; Leung, L. M. *Macromolecules* **1992**, *25*, 6195−6204.
(12) Wang, C. B.; Cooper, S. L. *Macromolecules* **1983**, *16*, 775−786.
(13) Yilgor, E.; Burgaz, E.; Yurtsever, E.; Yilgor, I. *Polymer* **2000**, *41*, 849−857.
(14) Valenkar, S.; Cooper, S. L. *Macromolecules* **2000**, *33*, 382−394.
(15) Woods, G. *The ICI Polyurethanes Book;* John Wiley and Sons: New York, 1990.
(16) Sun, H. *Macromolecules* **1993**, *26*, 5924−5936.
(17) Keuleers, R.; Desseyn, H. D.; Rousseau, B.; Van Alsenoy, C. *J. Phys. Chem. A* **1999**, *103*, 4621−4630.
(18) Furer, V. L. *J. Mol. Struct.* **2000**, *520*, 117−123.
(19) Flory, P. J. *Statistical Mechanics of Chain Molecules*; Wiley-Interscience: New York, 1969; reprinted by Hanser, Munchen, 1989.
(20) Mattice, W. L.; Suter, U. W. *Conformational Theory of Large Molecules*; Wiley-Interscience: New York, 1994.
(21) Gaussian 98, Revision A.6: Frisch, M. J.; Trucks, G. W.; Schlegel, H. B.; Scuseria, G. E.; Robb, M. A.; Cheeseman, J. R.; Zakrzewski, V. G.; Montgomery, J. A., Jr.; Stratmann, R. E.; Burant, J. C.; Dapprich, S.; Millam, J. M.; Daniels, A. D.; Kudin, K. N.; Strain, M. C.; Farkas, O.; Tomasi, J.; Barone, V.; Cossi, M.; Cammi, R.; Mennucci, B.; Pomelli, C.; Adamo, C.; Clifford, S.; Ochterski, J.; Petersson, G. A.; Ayala, P. Y.; Cui, Q.; Morokuma, K.; Malick, D. K.; Rabuck, A. D.; Raghavachari, K.; Foresman, J. B.; Cioslowski, J.; Ortiz, J. V.; Stefanov, B. B.; Liu, G.; Liashenko, A.; Piskorz, P.; Komaromi, I.; Gomperts, R.; Martin, R. L.; Fox, D. J.; Keith, T.; Al-Laham, M. A.; Peng, C. Y.; Nanayakkara, A.; Gonzalez, C.; Challacombe, M.; Gill, P. M. W.; Johnson, B.; Chen, W.; Wong, M. W.; Andres, J. L.; Gonzalez, C.; Head-Gordon, M.; Replogle, E. S.; Pople, J. A. Gaussian, Inc., Pittsburgh, PA, 1998.
(22) Mark, J. E.; Flory, P. J. *J. Am. Chem. Soc.* **1966**, *88*, 3702−3714.
(23) Flory, P. J. *Macromolecules* **1974**, *7*, 381−392.
(24) Calculations of the characteristic ratio of the PEU chain above have shown that the value $C_\infty = 5.0$ for the single block is the same as that for several blocks, and therefore the assumption of long chains in deriving eq 13 is fulfilled.
(25) Munson, B. R.; Young, D. F.; Okiishi, T. H. *Fundamentals of Fluid Mechanics*, 3rd ed.; Wiley: New York, 1998.

MA021217B